Kinetics of Surface Segregation and the Approach to Wetting in an Isotopic Polymer Blend

M. Geoghegan,[†,‡] T. Nicolai,[†,§] J. Penfold,[‖] and R. A. L. Jones*[,†]

Cavendish Laboratory, University of Cambridge, Cambridge CB3 0HE, U.K., and
Rutherford Appleton Laboratory, Chilton, Didcot, Oxfordshire OX11 0QX, U.K.

Received March 14, 1996; Revised Manuscript Received October 21, 1996[⊗]

ABSTRACT: We have used neutron reflectometry to study the kinetics of the formation of a surface-enriched layer of deuterated polystyrene from a film of a blend with normal (hydrogenated) polystyrene. Three blends are considered: one using a completely miscible blend and two approaching the coexistence curve from the one-phase region. A simple theory based upon the assumption that the surface-enriched layer is in local equilibrium with a depletion layer provides qualitative agreement with the data. The formation of a wetting layer "depinned" from the surface layer is not observed in the times studied in the experiment.

Introduction

If a thin film of a polymer blend is quenched into the two-phase region of the phase diagram, the influence of interfaces may profoundly modify the mechanisms of phase separation. The possibility that such surface-driven phase separation mechanisms, including the growth of wetting layers, could lead to useful self-assembled morphologies in thin polymer films has recently attracted considerable attention.[1] Of course, wetting phenomena are universal in all liquid mixtures, but the wetting behavior of polymer mixtures presents some unusual and interesting features. First, the unusual nature of polymer mixing thermodynamics leads to the prediction that even small differences in surface energy should drive a substantial surface segregation in single-phase mixtures and should lead to a surface phase diagram with a wetting transition rather far from criticality.[2,3] This means that the situation in which the lower surface energy phase of a two-phase polymer blend completely wets the surface (or a wall), rather than forming lenses with a finite contact angle, is expected to be much more common for polymer mixtures than it is for small molecule liquid mixtures. Thus the normal mechanism by which surfaces or interfaces promote phase separation in a mixture quenched into the metastable region of the phase diagram, heterogeneous nucleation, is replaced by a nonactivated mechanism in which a uniform wetting layer grows at the surface of the mixture. For deeper quenches, similar surface energy considerations lead to the phenomenon of surface-directed spinodal decomposition, in which the breaking of translational symmetry by a surface causes a composition wave to propagate from the surface of a polymer mixture into the bulk.[1,4,5] These new mechanisms of phase separation are particularly important for polymer thin films, and the unusual morphologies formed may well be useful in a variety of commercial areas, including the manufacture of asymmetric membranes and the preparation of coatings and films with optimized surface properties.

Another difference between polymers and small molecules is that diffusion of entangled polymer molecules is very slow. This means that the processes by which equilibrium is reached are all the more relevant, but also it allows one to study these kinetics conveniently.

Mixtures of hydrocarbon polymers with their deuterated analogues have proved particularly interesting;[6−15] their mixing thermodynamics is relatively simple,[16] and the deuterated component provides ideal contrast with the hydrogenated component for neutron reflectometry and some ion beam methods. The small difference in polarizability between the C−D and C−H bonds means that the deuterated component has a slightly smaller surface energy (excepting situations where the hydrogenated component is of a significantly lower molecular weight)[11] and preferentially segregates to the surface. Much work has focused on the size of the surface-segregated layer, with the adsorbed amount compared with that predicted by mean field theory to determine a bare surface energy difference between the two polymers. Specific differences between the surface profile predicted from mean field theory and that obtained experimentally have been discussed.

In this paper we turn our attention to the kinetics of the growth of a surface-enriched layer. For a miscible blend, it has been seen that a simple theoretical model, in which the surface-enriched layer, and its depletion layer, are approximated by discrete separate layers, is adequate to describe the growth of the surface layer.[8] On the other hand, in the two-phase part of the phase diagram, when the composition is held at one of its coexisting values by means of a reservoir of material at the other coexisting value, the same kind of model leads to the prediction of logarithmic growth of a wetting layer, as seen in experiments.[17]

Here we examine the very early stages of a surface-driven phase separation process in a model polymer mixture quenched into a part of the phase diagram close to the coexistence curve, using the technique of neutron reflectometry to probe the growth of a layer of the lower surface energy phase. The results of the experiments are then compared with calculations based on a simple theory that assumes diffusion-limited growth of a wetting layer. We also examine data on a miscible blend where we discuss the kinetics of the growth of a surface-enriched layer, away from wetting phenomena.

[†] Cavendish Laboratory.

[‡] Present address: Fakultät für Physik, Universität Freiburg, Hermann Herder Strasse 3, 79104 Freiburg, Germany.

[§] Present address: Laboratoire de Chimie et Physicochimie Macromoléculaire, Université du Maine, 72017 Le Mans Cedex, France.

[‖] Rutherford Appleton Laboratory.

[⊗] Abstract published in *Advance ACS Abstracts,* June 1, 1997.

S0024-9297(96)00394-4 CCC: $14.00

Table 1. Characteristics of the Polymers Used in the Present Study

polymer M_w	M_w/M_n (d-PS)	M_w/M_n (h-PS)
1 030 000	1.07	1.05
1 950 000	1.14	1.04

Experimental Section

We used two polymer blends: one in which both polystyrenes had a molecular weight (M_w) of 1.03×10^6 and another in which they both were of $M_w = 1.95 \times 10^6$. The polymers were anionically synthesized by Polymer Laboratories, and the polydispersity indices are listed in Table 1. Films were created by spin coating the polymer from a toluene solution onto 5 cm silicon wafers. The films were between 0.5 and 1 μm thick, enough to ensure that, for the annealing times used, finite size effects were not important. The films were annealed under vacuum, or in an argon atmosphere, at 457 K (184 °C) for times of up to 10 days. In these films d-PS segregated to the vacuum (or argon) interface, but a test using the direct depth-profiling technique of nuclear reaction analysis showed that there was no preferential d-PS segregation to the (unetched) silicon substrate.

The CRISP time-of-flight neutron reflectometer[18] of the ISIS spallation source at the Rutherford Appleton Laboratory was used for the reflection experiments. Data were obtained at two or three angles (usually 0.25, 0.5, and 0.8°); the higher angle data were obtained if the film was reflecting neutrons enough to keep the data above the background level. The analysis of neutron reflection data, and the technique itself, are described in detail elsewhere.[19,20] We used a downhill simplex algorithm to fit our neutron data to a model profile, as previously described by Jones *et al.*[21]

Theory

Surface Segregation and Wetting. We start by making calculations of the expected surface behavior of the two systems in question. Let us first consider the expected bulk phase diagram for the two systems. These may be calculated by standard methods[22] by assuming a value for the Flory–Huggins interaction parameter, χ, measured by neutron scattering:[16]

$$\chi = \frac{0.2}{T} - 0.00029 \tag{1}$$

where T, the temperature, is given in Kelvin and so χ has a value of 1.48×10^{-4} at 457 K. We have used a lattice volume, based on polystyrene, of 175 Å^3; the difference in the monomer volume of d-PS and h-PS is small enough to be neglected here. For the case of the blend with $M_w = 1.03 \times 10^6$, the critical point is expected to be at 400 K; thus, this system at experimental conditions is certainly in the one-phase region of the phase diagram. The predicted phase diagram for the blend with $M_w = 1.95 \times 10^6$ is shown in Figure 1; the critical point here is at 499 K. In addition to the uncertainty in the position of the coexistence curve arising from the measured value of χ, we must also recognize that limitations in the validity of the Flory–Huggins theory itself will arise in further uncertainties in the position of the coexistence curve. We see that one blend lies very close to the coexistence curve, and we cannot say, within error, on which side it falls.

The expected profiles near the surface may be calculated using the expression derived on the basis of square gradient theory.[2] The qualitative result for the $M_w = 1.03 \times 10^6$ case is straightforward; one expects a monotonic profile of the type considered by Jones *et al.*[6]

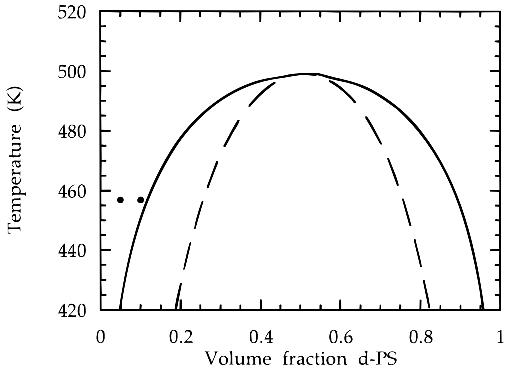

Figure 1. Predicted phase diagram for the blend with $M_w = 1.95 \times 10^6$. The full line is the binodal, and the broken line is the spinodal. The two d-PS concentrations used in this experiment are also shown.

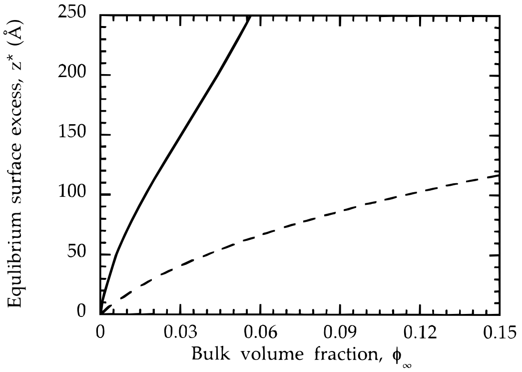

Figure 2. Adsorption isotherm, calculated at 457 K, for the $M_w = 1.03 \times 10^6$ (broken line) and $M_w = 1.95 \times 10^6$ (full line) blends. We have used a surface energy of $\Delta\gamma = 0.12$ mJ m^{-2} to calculate both of the adsorption isotherms.

A useful quantity to focus on is the surface excess, defined as

$$z^* = \int_0^\infty (\phi(z) - \phi_\infty)\, \mathrm{d}z \tag{2}$$

where z is the depth from the surface, $\phi(z)$ is the d-PS volume fraction at depth z, and ϕ_∞ is the bulk d-PS volume fraction. Figure 2 shows this as a function of the bulk volume fraction for the case of the $M_w = 1.03 \times 10^6$ system. We will need this function when we discuss our kinetic model. In order to calculate the curves shown in Figure 2, we take the surface volume fraction of this miscible blend at equilibrium and solve for z^* as a function of ϕ_∞ using[6]

$$z^* = \frac{l}{6}\int_{\phi_1}^{\phi_\infty} \frac{(\phi - \phi_\infty)\, \mathrm{d}\phi}{\sqrt{G(\phi) - G(\phi_\infty) - (\phi - \phi_\infty)\Delta\mu_\infty}} \tag{3}$$

where ϕ_1 is the surface volume fraction, b is the lattice parameter, l is the Kuhn statistical segment length, k_B is Boltzmann's constant, G is the Gibbs free energy of mixing (we use the usual Flory–Huggins form), and $\Delta\mu_\infty$ is the exchange chemical potential evaluated at the bulk volume fraction.

The situation is rather different for the case of the $M_w = 1.95 \times 10^6$ system. On the coexistence curve, the surface is expected to be completely wetted by a d-PS-rich layer; that is to say, a d-PS-rich layer of divergent thickness is expected to intrude between the vacuum and the bulk (of course, in real systems, the thickness is limited by one or more of gravity, finite total film thickness, or kinetic effects). We estimate that for our higher molecular weight blend we are well above the temperature corresponding to the wetting transition.[3]

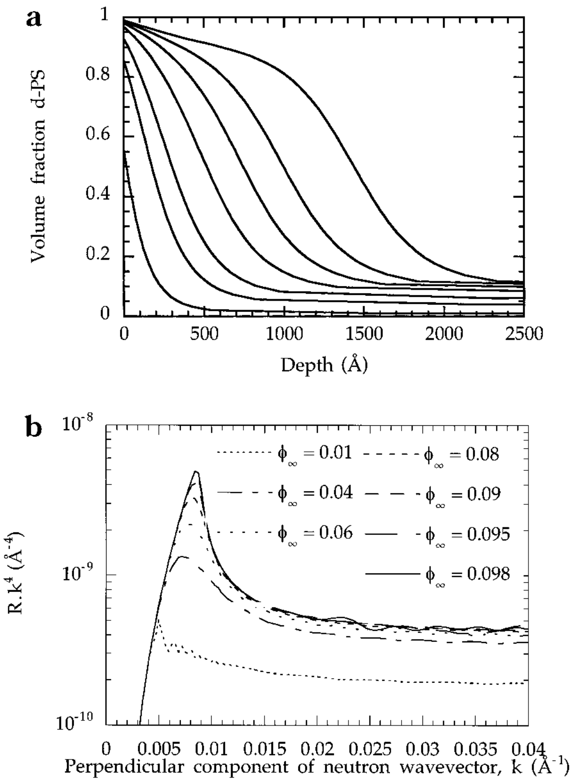

Figure 3. (a) Model calculations showing equilibrium surface profiles for bulk concentrations, ϕ_∞, of 0.01, 0.04, 0.06, 0.08, 0.09, 0.095, and 0.098. The curves may be identified simply by noting that the surface excess and surface volume fraction increase monotonically, with $\phi_\infty = 0.01$ being the smallest for both parameters and 0.098, the largest. The binodal volume fraction is 0.10, corresponding to a temperature of 450 K for a blend of d-PS and h-PS. The surface energy used is that obtained for the fully miscible blend, 0.12 mJ m^{-2}. It is clear that for the two largest values of ϕ_∞ that a wetting layer has depinned from the surface. (b) Neutron reflectivity simulations of the above profiles for 5000 Å thick films on silicon plotted as Rk^4. As complete wetting is reached, it becomes more difficult to differentiate the simulations, with those for $\phi_\infty =$ 0.090, 0.095, and 0.098 barely distinguishable.

As one approaches the coexisting composition by changing the composition at constant temperature, the profiles gradually change from the monatonic profiles expected in the one-phase region to profiles with the inflection characteristic of the approach to wetting. Figure 3a shows model calculations of the composition profile (simulated reflectivity profiles are shown in Figure 3b) for the high M_w blend for various bulk volume fractions, and the adsorption isotherm for this blend is included in Figure 2, where we have used the same surface energy in the calculation as for the lower M_w blend. (This calculation for the surface energy is described in the Results and Discussion, and it enables us to calculate the equilibrium surface volume fraction for a given bulk volume fraction.) These profiles were obtained from[2]

$$z = \frac{l}{6}\int_{\phi_1}^{\phi_\infty} \frac{d\phi}{\sqrt{G(\phi) - G(\phi_\infty) - (\phi - \phi_\infty)\Delta\mu_\infty}} \qquad (4)$$

The surface excess is expected to diverge logarithmically on the binodal[23] for the case where the forces driving surface segregation (i.e., the difference in surface energy between the components) are short ranged. Again, we will need this result when we come back to discuss the kinetic model.

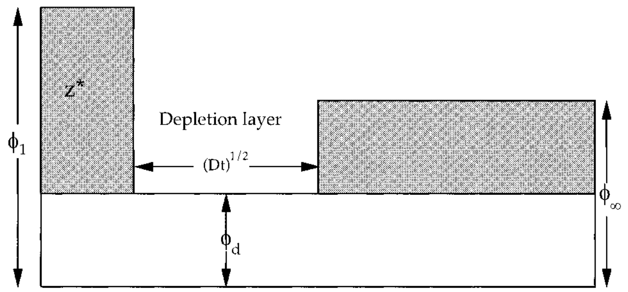

Figure 4. Schematic diagram representing the simple model of Jones and Kramer.[8]

Calculations of the Growth Law. A full theory of the kinetics by which a polymer wetting layer grows has not yet been presented. Binder and Frisch[24] have proposed a theory for a related situation, but the dynamics of the system they studied are not expected to be the same as in the polymer case. At early stages, internal chain dynamics are likely to be important, but later one might expect the growth of the layer to be controlled by the rate of diffusion of chains from the bulk of the material to the surface. A simple, phenomenological approach due to Lipowsky and Huse[25] uses this idea and proposes that one can consider a local equilibrium between the surface layer and a region locally depleted in the surface active polymer behind the surface layer. The model treats the surface and depletion layers as separate. The surface layer is a function of the depletion layer volume fraction. If one knows the volume fraction of the depletion layer, one can equate it to the bulk volume fraction at equilibrium (this is the local equilibrium assumption) and calculate the surface segregation profile as given by eq 4. At time $t = 0$ the depletion layer has a volume fraction $\phi = 0$. This represents a sharp concentration gradient with respect to the bulk and must relax by interdiffusion. As the depletion layer volume fraction increases due to the relaxation of this concentration gradient, so the size of the surface-segregated layer must also increase, since it must be in equilibrium with the depletion layer. The surface profile is thus a consequence of the growth of the depletion layer, and its growth is therefore controlled by the interdiffusion coefficient at the depletion layer volume fraction. We are taking a liberty with our model by starting at $t = 0$ since, as we have said, internal chain dynamics are important at this point, and our model only becomes valid when the growth is diffusion limited.

Figure 4 shows the picture envisaged. In the case where the bulk is in the stable one-phase region, this type of model predicts an initial growth with characteristic diffusion $\sqrt{t}$ kinetics with time, saturating after a time of order

$$t_{eq} \approx \left(\frac{z_{eq}^*}{\phi_\infty}\right)^2 \frac{1}{D} \qquad (5)$$

to the equilibrium surface excess z_{eq}^*, where D is the interdiffusion coefficient. More precisely, one may solve the diffusion equation numerically with a partially reflecting boundary condition at the surface, which ensures that the condition of local equilibrium is met. This approach has been tested experimentally for a blend of d-PS and h-PS, and quantitative agreement is found between theory and experiment, using the known value of the interdiffusion coefficient for the system.[8]

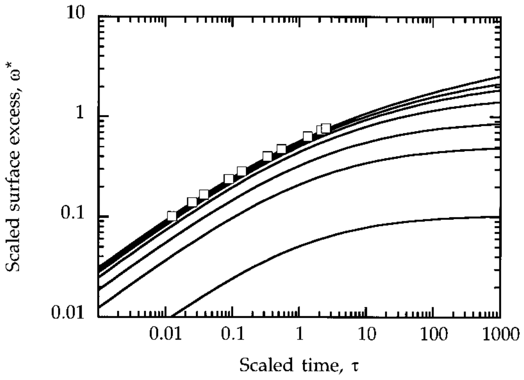

Figure 5. Surface excess with time for various values of ϕ_∞/ϕ_α. These correspond to the same systems as in Figure 3 (except that we have replaced $\phi_\infty = 0.098$ with the binodal value, $\phi_\infty = 0.10$), again with the smallest values of ω^* due to $\phi_\infty = 0.01$ ($\phi_\infty/\phi_\alpha = 0.10$) and the largest due to $\phi_\infty = 0.10$ ($\phi_\infty/\phi_\alpha = 1.0$). The rescaled time and surface excess are discussed in the text. We have also included results of a numerical solution to the diffusion equation for $\phi_\infty/\phi_\alpha = 1.0$ and see that they fall on the curve for the simple model of Jones and Kramer.[8]

In the case of a blend with the preferentially segregating component at, or near, coexistence, the situation is somewhat different. Initially, the surface layer will grow with diffusion-limited $\sqrt{t}$ kinetics, but as the value of ϕ_d approaches the coexistence value, ϕ_α, the surface excess begins to diverge logarithmically. If $\phi_\infty > \phi_\alpha$, there will be a final stage where $\sqrt{t}$ kinetics return. We can see this by considering the mathematics of the model. First we write the law governing the growth of the surface excess,

$$z^* = (\phi_\infty - \phi_d(t))\sqrt{Dt} \tag{6}$$

This is a simple statement of the local equilibrium approximation for diffusion-limited kinetics. We note the logarithmic growth of the surface excess near coexistence:

$$z^* = -a \ln\left(\frac{\phi_\alpha - \phi_d}{\phi_\alpha}\right) \tag{7}$$

which we can substitute into eq 6 to obtain

$$z^* = (\phi_\infty - \phi_\alpha(1 - e^{-z^*/a}))\sqrt{Dt} \tag{8}$$

where a is a constant. To illustrate this, Figure 5 shows the growth ($\sqrt{t}$) of surface layers for different values of ϕ_∞. We have facilitated analysis by scaling the surface excess by z^*/a and the time by $\phi_\alpha^2 Dt/a^2$. Equation 8 thus reduces to

$$\omega^* = \tau^{0.5}\left(\frac{\phi_\infty}{\phi_\alpha} + e^{-\omega^*} - 1\right) \tag{9}$$

where ω^* and τ are the scaled surface excess and time, respectively.

At this point we should consider three possible limitations of this analysis. First, there is the question of how good an approximation to the full solution of the diffusion equation our approach of using a structure based on three discrete layers can be. We have tested this assumption by numerically solving the diffusion equation with appropriate boundary conditions for some parameter values. This is illustrated in Figure 5. Here we show various predictions of the simple model by varying ϕ_∞/ϕ_α. We see that the value of ϕ_∞/ϕ_α is more significant at later times. The full numerical solution of this equation is included for one value of ϕ_∞/ϕ_α and shows excellent agreement with our simple model. We therefore believe that approximating the diffusion profile to a series of discrete layers is sufficiently accurate for our purposes. We must also consider the validity of eq 7 for polymer mixtures. Although this equation correctly describes the divergence of the surface excess approaching coexistence, it does not accurately describe the surface excess for concentrations significantly lower than coexistence. A more careful analysis must use a parametrized form of the adsorption isotherm as calculated numerically from the square gradient theory. We have done this in our data analysis, though it should be noted that the effects of this refinement are quantitative rather than qualitative. Finally, one must also remember that the diffusion coefficient is composition dependent, particularly as one approaches the spinodal where thermodynamic slowing down becomes important (the value of D on the spinodal falls to zero and, for our isotopic blend, varies like $1 - 2\phi(1 - \phi)\chi N$, where N is the chain length, according to mean field theory).[26] In our experiments, however, the interdiffusion coefficient is not expected to vary by more than a factor of 2, at most.

Results and Discussion

The data and fits are included in Figure 6, and the corresponding depth profiles are shown in Figure 7. Depending on the neutron detector used, there were differing backgrounds in the experiments; to aid clarity, we have subtracted the background from the data. Incoherent scattering by hydrogen was accounted for by the inclusion of an imaginary part in the scattering length density of h-PS.[21] All data were fitted to error functions, except the 30 min data shown in Figures 6b and 7b. Of course, the diffusion-limited model would predict a near surface composition profile, which combines a depletion layer obtained from the numerical solution to the diffusion equation with the surface segregation profile calculated from mean field theory by assuming a bulk composition corresponding to the depleted composition ϕ_d. However, an error function, with its adjustable width and offset, allows us much greater freedom to fit the data; in any case, we know that there are systematic discrepancies in the details of the profile shape between mean-field predictions and the results of experiments.[10,27,28] Certainly, the theoretical mean field profile, which resembles an exponential decay, has been shown to be inadequate for blends of d-PS and h-PS.[10] NR is also insensitive to shallow gradients such as might be found where the depletion layer increases with depth from its lowest volume fraction to the bulk value. We therefore gain no further information from fitting to a model that includes a depletion layer. The measured surface excess is slightly less than the true surface excess because of the absence of a depletion layer in our model, but this underestimation decreases with increasing annealing time.

The data for the 30 min sample shown in Figure 6b could not be fitted by the error function profile; instead, it was necessary to include a thin layer of d-PS at the surface. A simple three-layer fit, with roughness between each layer, was used in this case. It may be that, in such a short annealing time, differences in the sample's approach to thermal equilibrium may alter the initial kinetics; this is discussed for another blend

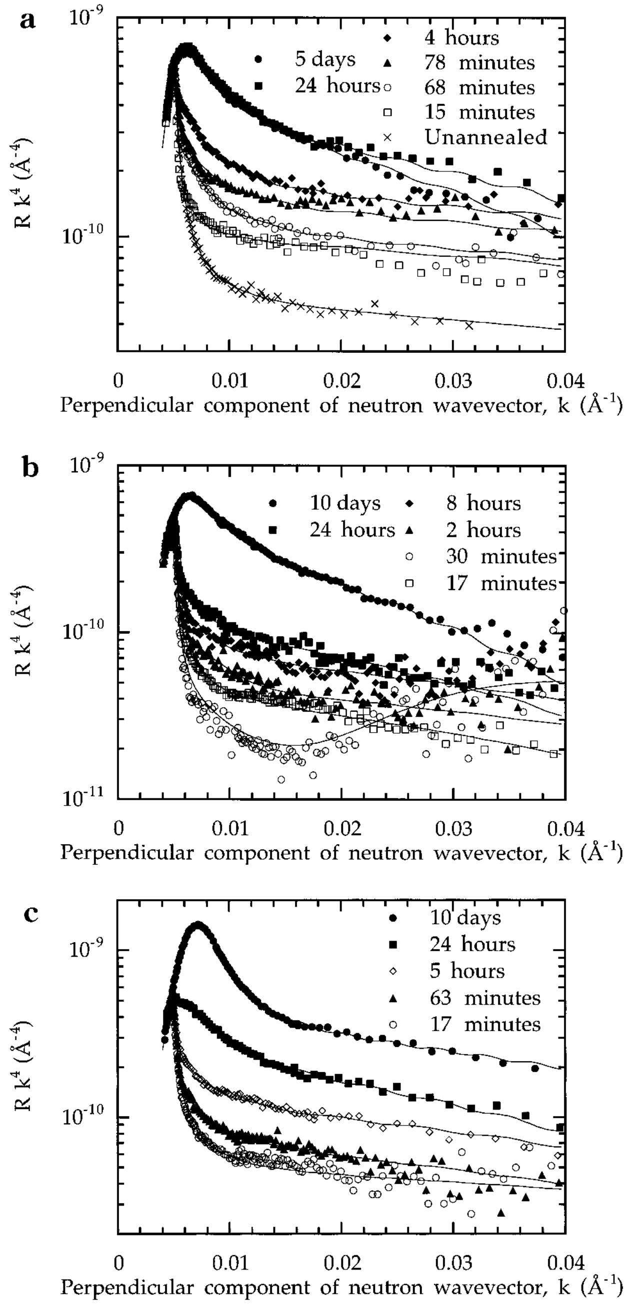

Figure 6. NR data and best fits for (a) the $M_w = 1.03 \times 10^6$ blend, (b) the $M_w = 1.95 \times 10^6$ blend with $\phi_\infty = 0.049$, and (c) the $M_w = 1.95 \times 10^6$ blend with $\phi_\infty = 0.10$. The values of χ^2 for the fits are (a) 1.2 (unannealed), 6.1 (15 min), 6.2 (68 min), 5.3 (78 min), 1.7 (4 h), 1.9 (24 h), and 1.8 (5 days), (b) 4.5 (17 min), 1.2 (30 min), 0.9 (2 h), 1.3 (8 h), 1.0 (24 h), and 2.9 (10 days), and (c) 2.7 (17 min), 3.2 (63 min), 2.8 (5 h), 3.3 (24 h), and 4.7 (10 days). The annealing temperature was 457 K.

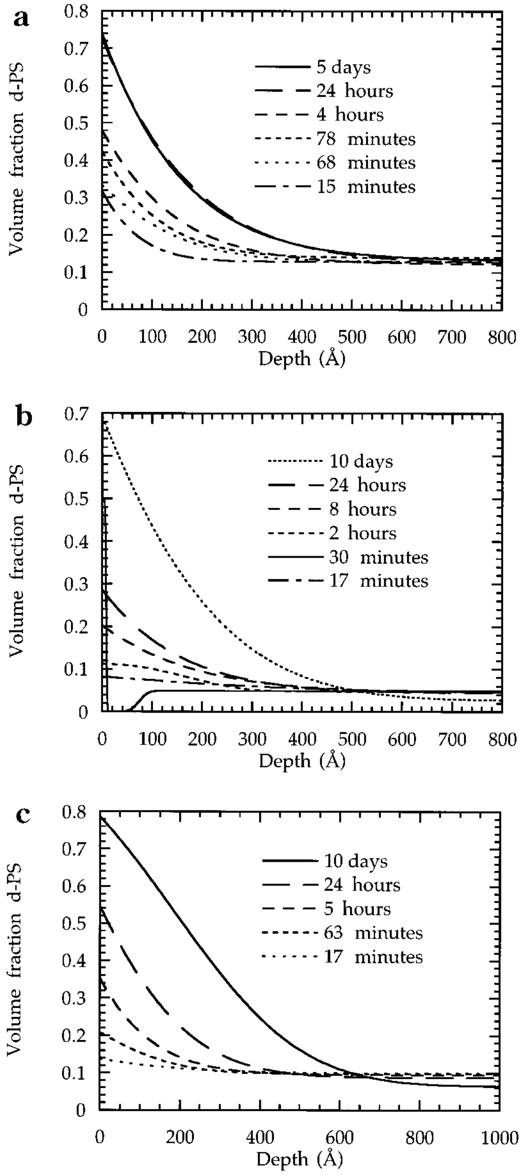

Figure 7. Corresponding volume fraction–depth profiles for the fits in Figure 6.

elsewhere.[27] At early times, our model is not applicable, since it concerns only diffusion-limited mass transport. The profile for this 30 min sample is one where transport to the surface is from the immediate vicinity of the surface rather than the bulk of the sample. That we see this for the 30 min sample and not in the 17 min data implies that the 30 min sample reached thermal equilibrium in the oven more slowly than the 17 min sample. For the 30 min sample, the reflectivity profile was sensitive to the back edge of the depletion layer and so it had to be included in the fit.

In all cases, surface roughness was included in the fitting. In the absence of surface roughness (and background), the asymptotic behavior of Rk^4, as shown in Figure 6, would be constant (Porod's law), as is the case in the simulations of Figure 3b. Surface roughness causes this asymptote to decrease with increasing wavevector and is easily extracted from the data. We approximate this behavior with a Gaussian roughness term in the fits. This is equivalent to either two-dimensional waves at the surface in the plain of the surface or a one-dimensional error function profile, which would contribute to the depth profile. The surface roughnesses are measured as between 8 and 20 Å, and we exclude them from the profiles in Figure 7.

Our first analysis of the data will be to consider the simple model of Jones and Kramer,[8] with the adsorption isotherm calculated from mean field theory. First we consider the miscible blend. We show, in Figure 8, the surface excess plotted against $\sqrt{t}$, and it is clear that in this time we are close to equilibrium. In Figure 7 we see that the decay length of the profile is comparable with the polymer radius of gyration (~260 Å), in agreement with other work on the isotopic polystyrene blend. We take the surface volume fraction of the 5 day profile and can use this to obtain a bare surface energy difference, $\Delta\gamma$, between the two polymers.[2] This is when

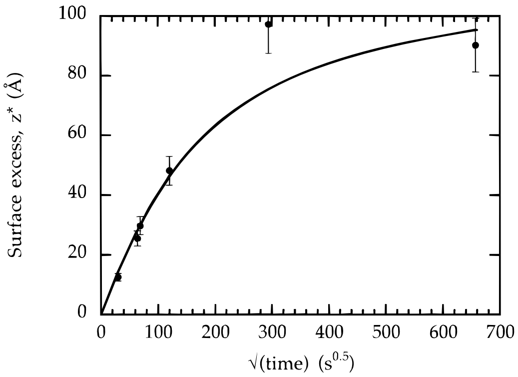

Figure 8. z^* against $\sqrt{t}$ for the 14% blend with $M_w = 1.03 \times 10^6$. The solid line is a fit to the simple model using the surface excess obtained from a mean field calculation ($\Delta\gamma = 0.12$ mJ m^{-2}). We obtain a diffusion coefficient of 1.1×10^{-15} cm^2 s^{-1}. The error bars represent a 10% error in the value of z^*.

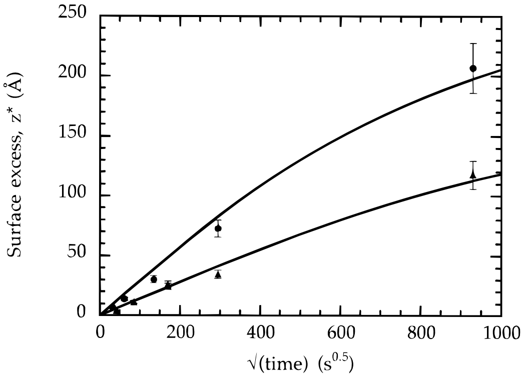

Figure 9. z^* against $\sqrt{t}$ for 5% (▲) and 10% (●) blends. The lines are fits to the data using a surface excess, $\Delta\gamma = 0.21$ mJ m^{-2}, and a diffusion coefficient of 8.3×10^{-16} cm^2 s^{-1}. The error bars are again 10% of the measured surface excess.

$$\frac{b^3\Delta\gamma}{k_B T} - b\chi\left(\phi_1 - \frac{1}{2}\right) = \frac{l}{3}\sqrt{\frac{G(\phi_1) - G(\phi_\infty) - (\phi_1 - \phi_\infty)\Delta\mu_\infty}{\phi_1(1 - \phi_1)}} \quad (10)$$

where b is the lattice parameter. We find that $\Delta\gamma = 0.12$ mJ m^{-2}, larger than the value of 0.08 mJ m^{-2} obtained by Jones *et al.* when considering a blend with d-PS and h-PS of $M_w = 1.03 \times 10^6$ and $M_w = 1.8 \times 10^6$, respectively.[6] Alternatively, we can also obtain a surface energy difference from our equilibrium measurement of z^*, rather than ϕ_1; this comes out as 0.10 mJ m^{-2}. From the surface energy, we can calculate the surface excess at various values of ϕ_d and thus produce an adsorption isotherm for substitution into eq 4. Also in Figure 8, we include the optimal fit with only one floating parameter, the diffusion coefficient. This is estimated to be 1.1×10^{-15} cm^2 s^{-1}. We may compare this with the diffusion coefficient interpolated to our temperature and molecular weight on the basis of reptation dynamics from the value measured by forward recoil spectrometry;[26] this is calculated to be 9×10^{-15} cm^2 s^{-1}. So, we conclude that simple mean field theory provides an adequate explanation of the kinetics of surface segregation, although we do reach equilibrium slightly more quickly than theory predicts.

Next we attempt to apply this model to the partially miscible blend. The results are shown in Figure 9. As we can see, at shorter annealing times, the agreement is very good, giving us an interdiffusion coefficient of 8.3×10^{-16} cm^2 s^{-1}, but to get agreement at longer annealing times, we would have to assume a surface energy difference of 0.21 mJ m^{-2}, some 75% larger than for the miscible system. This difference seems implausible, as surface energy is a very weak function of molecular weight for high polymers.[29]

Nor does the value of the interdiffusion coefficient obtained from our data scale with that predicted by theory, taking into account both the decrease in mobility predicted by reptation for increasing molecular weight and the effect of thermodynamic slowing down, which is affected by both the difference in molecular weights and the difference in bulk volume fractions. Previous results on d-PS/h-PS blends suggest that our miscible blend should have an interdiffusion coefficient of around 9×10^{-15} cm^2 s^{-1}, whereas that for the partially miscible blend is expected to be around 3×10^{-15} cm^2 s^{-1}.[27] Instead of this factor of 3 reduction in D, for a factor of 2 increase in M_w, we see the diffusion coefficient decreases from 1.1×10^{-15} cm^2 s^{-1} to 8.3×10^{-16} cm^2 s^{-1}. This may in part be explained by the value of the interaction parameter. We turn to the question of the interaction parameter below. Even so, changing the interaction parameter does not allow us to explain these results. However, thermodynamic slowing down must play a large part in the explanation of this behavior; with the interdiffusion coefficients we use, we calculate that, with $\phi_\infty = 0.35$ and $\phi_\infty = 0.05$ for the miscible and partially miscible blends, respectively, there is only a 25% decrease in the interdiffusion coefficient when one changes M_w from 1.03×10^6 to 1.95×10^6. It is possible that a failure of simple Flory–Huggins theory to predict quantitatively the effect of thermodynamic slowing down, in the same way that it does not reproduce the exact shape of the coexistence curve, may partially account for this discrepancy.

We have used the Bates and Wignall interaction parameter[16] in all of our analysis. We now comment on the effect of using other measurements of the interaction parameter by Green and Doyle[26]

$$\chi = \frac{0.22}{T} - 0.00032 \quad (11)$$

and that by Budkowski *et al.*:[13]

$$\chi = \left(\frac{0.124}{T} - 0.000106\right)(1 - 0.18\phi) \quad (12)$$

The position of the phase boundary for the partially miscible blend moves from (0.117, 0.257) for the χ determined by Bates and Wignall to (0.084, 0.226) (Green and Doyle) and to (0.079, 0.199) (Budkowski *et al.*), where the first number in parentheses is the coexistence value and the second is the spinodal. The effect on the miscible blend is negligible. Both parameters are larger than that of Bates and Wignall at 457 K. However, the largest, that of Budkowski *et al.*, only causes a drop in surface energy from $\Delta\gamma = 0.12$ to 0.11 mJ m^{-2}. Similarly, there is very little effect on the diffusion coefficients, which are tabulated in Table 2. For the partially miscible blend, there is more of an effect on the diffusion coefficient but the lowest value calculated is still more than 60% of the highest value at the same volume fraction ($\phi = 0.10$). We note from Figure 2 that, for a surface excess corresponding to the maximum that we have measured (207 Å), the volume fraction is a little over 0.04. In other words, the depletion layer is never particularly far away from $\phi =$

Table 2. Values of the Interdiffusion Coefficient Calculated for the Values of χ Given by Bates and Wignall (BW)[16] (Eq 1), Green and Doyle (GD)[26] (Eq 11), and Budkowski *et al.* (BSK)[13] (Eq 12)

	interdiffusion coefficient (10^{-15} cm^2 s^{-1})											
	$\phi = 0$			$\phi = 0.05$			$\phi = 0.10$			$\phi = 0.14$		
blend (M_w/M_w)	BW	GD	BSK	BW	GD	BSK	BW	GD	BSK	BW	GD	BSK
1 030 000/1 030 000	14	14	14							9	9	7
1 950 000/1 950 000	3.8	3.8	3.8	2.8	2.7	2.3	1.9	1.8	1.2			

0, and so this further limits the effect of χ on the diffusion coefficient. The reason that we are not affected so much in these calculations by the different values of χ is that the interdiffusion coefficient falls to zero on the spinodal, and not on the coexistance curve. We are still some distance away from the spinodal, whichever value of χ we use.

Another shortcoming of the kind of theory discussed so far in this account is the assumption of a short range, δ-function, surface interaction. However, we know that the surface energy of essentially nonpolar polymers, such as polystyrene, arises from intermolecular van der Waals forces, which are intrinsically long ranged. For the surface segregation of miscible polymers, it has been shown that the effect on the equilibrium profiles of approximating the interactions by short range forces is negligible; however, as coexistence is approached, the differences become more substantial.[30] The logarithmic divergence of z^* predicted for the case of short range forces is replaced in the case of van der Waals forces by a divergence in z^*, which goes as $\Delta\mu_\alpha{}^{-1/3}$. This effect may start to be significant in the $\phi_\infty = 0.10$ blend, especially if χ is slightly larger than the value we have used here. The early time results would not be affected (ϕ_d is too far from coexistence), but at the longest times z^* should increase relative to our analysis.

It should be stressed, however, that for the annealing times we have used, we do not see the growth of a fully-fledged wetting layer. The 10% data show that, for the sample annealed for 10 days, a point of inflection has appeared in the near-surface profile. This is the signature of the incipient wetting layer starting to become depinned from the interface, but in this case, the surface volume fraction has still not reached the upper coexistence value so the wetting layer has not fully formed at this point. The simulations in Figure 3b show that the growth of the wetting layer is not easily followed by NR for this system; a more immiscible system, however, with a more pronounced interface would provide fringes, from which we could determine the thickness of the wetting layer.

We have seen in experiments on a blend of d-PS and poly(α-methylstyrene)[26] that in films quenched into the metastable region of the phase diagram, the growth of the wetting layer is affected by the existence of phase-separated domains in the bulk of the film, which act as nucleation points, depleting the matrix of d-PS and inhibiting the wetting layer growth. We do not believe that this is a problem in these experiments because the diffusion coefficient of the polystyrene is too small for there to be significant nucleation. We also note that the unannealed miscible film was easily fitted to a homogeneous profile; the experiment was not performed for an unannealed partially miscible film, but the lack of significant enrichment for the shorter annealing times indicates that any segregation is negligible. The absence of surface segregation in unannealed films means that there is unlikely to be any nucleation in the bulk (since the surface is an efficient nucleation site).

Summary

We have used neutron reflectometry to study the surface segregation of d-PS at the surface of blends of high molecular weight d-PS and h-PS. For blends close to the coexistence curve, quite large amounts of d-PS are segregated to the surface with rather slow kinetics. We have interpreted these results as indicating an approach to complete wetting of the surface by a d-PS rich phase. We have analyzed the data using a simple model based on mean field theory together with the assumption of local equilibrium between the surface and depletion layers. This model gives qualitative agreement with mean field theory, but we reveal limitations of this analysis and make suggestions as to possible reasons for some of the discrepancies.

The kinetics of surface segregation for a completely miscible lower molecular weight blend are in reasonable agreement with theory. Although the detailed profile shape is not exactly that predicted by mean field theory, we have used mean field theory to estimate the surface energy difference between the components of the blend as $\Delta\gamma = 0.11 \pm 0.02$ mJ m^{-2}, in reasonable agreement with other results on similar systems.

Assuming a similar surface energy difference in a higher molecular weight, partially miscible blend, we find good agreement with mean field theory at early times. There is the possibility that van der Waals forces are responsible for the discrepancy at later times for a quench deeper into the metastable part of the phase diagram.

A notable anomaly in our results is that the diffusion coefficient needed to fit our data well fell by only about 25% when we used polymers of double the molecular weight. This partly reflects the details of the effect of thermodynamic slowing down on the diffusion coefficient when both the molecular weight and the volume fraction are changed, but also probably highlights a large error due to the limits on our knowledge of the precise location of the coexistence curve.

Acknowledgment. This work was supported by the AFRC, the SERC, and ICI Plc. We thank Mrs. Frances Nex for performing some computations.

References and Notes

(1) Krausch, G. *Mater. Sci. Eng. Rep. R* **1995**, *14*, 1.
(2) Schmidt, I.; Binder, K. *J. Phys.* **1985**, *46*, 1631.
(3) Jones, R. A. L. *Polymer* **1994**, *35*, 2160.
(4) Ball, R. C.; Essery, R. L. H. *J. Phys.: Condens. Matter* **1990**, *2*, 10303.
(5) Jones, R. A. L.; Norton, L. J.; Kramer, E. J.; Bates, F. S.; Wiltzius, P. *Phys. Rev. Lett.* **1991**, *66*, 1326.
(6) Jones, R. A. L.; Kramer, E. J.; Rafailovich, M. H.; Sokolov, J.; Schwarz, S. A. *Phys. Rev. Lett.* **1989**, *62*, 280.
(7) Jones, R. A. L.; Kramer, E. J.; Rafailovich, M. H.; Sokolov, J.; Schwarz, S. A. *Mater. Res. Soc. Symp. Proc.* **1989**, *153*, 133.
(8) Jones, R. A. L.; Kramer, E. J. *Philos. Mag. B* **1990**, *62*, 129.
(9) Composto, R. J.; Stein, R. S.; Jones, R. A. L.; Kramer, E. J.; Felcher, G. P.; Karim, A.; Mansour, A. *Physica B* **1989**, *157–158*, 434.

(10) Jones, R. A. L.; Norton, L. J.; Kramer, E. J.; Composto, R. J.; Stein, R. S.; Russell, T. P.; Mansour, A.; Karim, A.; Felcher, G. P.; Rafailovich, M. H.; Sokolov, J.; Zhao, X.; Schwarz, S. A. *Europhys. Lett.* **1990**, *12*, 41.
(11) Hariharan, A.; Kumar, S. K.; Russell, T. P. *J. Chem. Phys.* **1993**, *98*, 4163.
(12) Hariharan, A.; Kumar, S. K.; Rafailovich, M. H.; Sokolov, J.; Zheng, X.; Duong, D.; Schwarz, S. A.; Russell, T. P. *J. Chem. Phys.* **1993**, *99*, 656.
(13) Budkowski, A.; Steiner, U.; Klein, J. *J. Chem. Phys.* **1992**, *97*, 5229.
(14) Hong, P. P.; Boerio, F. J.; Smith, S. D. *Macromolecules* **1993**, *26*, 1460.
(15) Hong, P. P.; Boerio, F. J.; Smith, S. D. *Macromolecules* **1994**, *27*, 596.
(16) Bates, F. S.; Wignall, G. D. *Macromolecules* **1986**, *19*, 932.
(17) Steiner, U.; Klein, J.; Eiser, E.; Budkowski, A.; Fetters, L. J. *Science* **1992**, *258*, 1126.
(18) Penfold, J.; Ward, R. C.; Williams, W. G. *J. Phys. E* **1987**, *20*, 1411.
(19) Penfold, J.; Thomas, R. K. *J. Phys.: Condens. Matter* **1990**, *2*, 1369.
(20) Russell, T. P. *Mater. Sci. Rep.* **1990**, *5*, 171.
(21) Jones, R. A. L.; Norton, L. J.; Shull, K. R.; Kramer, E. J.; Felcher, G. P.; Karim, A.; Fetters, L. J. *Macromolecules* **1992**, *25*, 2359.
(22) de Gennes, P. G. *Scaling Concepts in Polymer Physics*; Cornell University Press: Ithaca, NY, 1979.
(23) Cahn, J. W. *J. Chem. Phys.* **1987**, *66*, 3667.
(24) Binder, K.; Frisch, H. L. *Z. Phys. B* **1991**, *84*, 403.
(25) Lipowsky, R.; Huse, D. A. *Phys. Rev. Lett.* **1986**, *57*, 353.
(26) Green, P. F.; Doyle, B. L. *Phys. Rev. Lett.* **1986**, *57*, 2407.
(27) Geoghegan, M.; Jones, R. A. L.; Sivia, D. S.; Penfold, J.; Clough, A. S. *Phys. Rev. E* **1996**, *53*, 825.
(28) Norton, L. J.; Kramer, E. J.; Bates, F. S.; Gehlsen, M. D.; Jones, R. A. L.; Karim, A.; Felcher, G. P.; Kleb, R. *Macromolecules* **1995**, *28*, 8621.
(29) Sauer, B. B.; Dee, G. T. *Macromolecules* **1991**, *24*, 2124.
(30) Jones, R. A. L. *Phys. Rev. E* **1993**, *47*, 1437.

MA9603948